

Generalized Damage Diagnostics of Two Miter Gates Through Domain Adaptation

GUOFENG QIAN, HAIWEI LIN, TRAVIS FILLMORE,
HAI NGUYEN, BRIAN EICK, ZHEN HU and MICHAEL TODD

ABSTRACT

Scarce monitoring data spanning unique civil infrastructure classes limits damage diagnostic generalization using data-driven approaches. While physics-based methods can address some limitations, they struggle to accurately simulate complex damage mechanisms, such as corrosion and fatigue cracks. To alleviate the data scarcity challenge, this study proposes generalizing diagnostic algorithms from structures with abundant data on condition and performance (source) to similar structures with little or not data (target). By leveraging diagnostic mappings through domain adaptation, it becomes possible to diagnose analogous structures within a class effectively. This research focuses on multi-damage diagnostics between two miter gates using an adversarial domain adaptation approach. Two types of damage are simulated using validated finite element models. Diagnostic knowledge from the source gate is transferred to the target gate, enabling accurate diagnostics despite the lack of labeled data for the latter. The results demonstrate that the proposed approach achieves reasonable accuracy in diagnosing unlabeled target structures, highlighting the feasibility of transferring diagnostic information across domains with similar label ranges.

INTRODUCTION

The mapping of damage characteristics obtained from measurements to the condition, a key step in diagnostics, can be effectively performed through through data-driven methods such as machine learning [1]. However, data scarcity poses a challenge since training data from all desired structural states is rarely available. If diagnostic algorithms can be generalized to detect damage from a group of similar structure, more useful information can be discerned from limited available data. Therefore, structural and damage

Guofeng Qian, Haiwei Lin, Michael D. Todd, Department of Structural Engineering, University of California at San Diego, 9500 Gilman Drive, La Jolla, CA 92093. Travis Fillmore, Coastal and Hydraulics Laboratory, U.S. Army Engineer Research and Development Center, Vicksburg, MS 39180. Hai Nguyen, Brian Eick, Construction Engineering Research Laboratory, U.S. Army Engineer Research and Development Center, Champaign, IL 61821. Zhen Hu, Department of Industrial and Manufacturing Systems Engineering, University of Michigan-Dearborn, 4901 Evergreen Rd, Dearborn, MI 48128. Corresponding author email: mdtodd@ucsd.edu

similarities can be utilized to overcome data scarcity. As human health diagnostics are based on shared fundamental biological similarities across all human beings, this proposal seeks to advance structural diagnostics to a similar population- or group-based level.

Prior research includes Population-Based SHM (PBSHM), which seeks to transfer information between structures using domain adaptation (DA) [2,3]. By adapting measurements from a less-studied structure (with no labeled data) to a well-studied structure (with labeled data), the diagnostic algorithm from well-studied structure can be applied directly. However, certain components of the measurement data might be more sensitive to the damage status than others. This information is neglected in direct adaptation between measurements, as the DA algorithm does not account for diagnostic mapping, potentially leading to negative transfer, which incorrectly maps information from one domain to another and reduces performance [2]. To avoid negative transfer, information transfer between structures should also be guided by diagnostic mapping.

While our ultimate objective is to generalize diagnostic algorithms across multiple similar structures, we begin with the simplest scenario: transferring knowledge from one structure to another. In the current study, we consider a well-studied structure equipped with sensors, where both sensor readings and associated damage states are available. A similar second structure is also instrumented with sensors; however, its damage status remains unlabeled. Leveraging structural and damage similarities between the two structures, our goal is to apply the relationship established between sensor measurements and damage labels from the first structure to predict the unknown damage conditions in the second.

THE FINITE ELEMENT MODELS AND SIMULATED STRAIN VALUES

This study focuses on two downstream miter gates: the Bonneville gate and the Dalles gate. Both gates are located in the Columbia River. The Bonneville gate, in service since 1993, is located approximately 40 miles east of Portland, Oregon, near North Bonneville, Washington [4], with approximate dimensions of 54 feet wide and 92 feet high. The Dalles gate, which has been in service since 2011, is located about two miles east of the city of The Dalles, Oregon [5,6], with approximate dimensions of 52 feet wide and 106 feet high. Maintaining both gates is critical not only to ensure the continuous flow of billions of dollars' worth of agricultural goods but also to uphold the economic stability of the entire Pacific Northwest region [7].

Finite element (FE) models of the Bonneville and Dalles miter gates were developed using ABAQUS. Fig. 1 presents schematic illustrations and the main structural components of both gates. The models employed linear elastic material properties to represent the behavior of steel. As the gates mainly consists of welded steel plates, the FE model predominantly employed linear four-node shell elements (S4R). Both gates were subjected to hydrostatic pressure to simulate the effects of upstream and downstream water loads. Gravity load is neglected in the simulation because it induces stable and relatively small deformations that remain essentially unchanged. The analysis focuses on strain differences driven by variable loads and damages, making the contribution of gravity negligible when computing strain changes.

Similar boundary conditions were applied to the two models: horizontal displace-

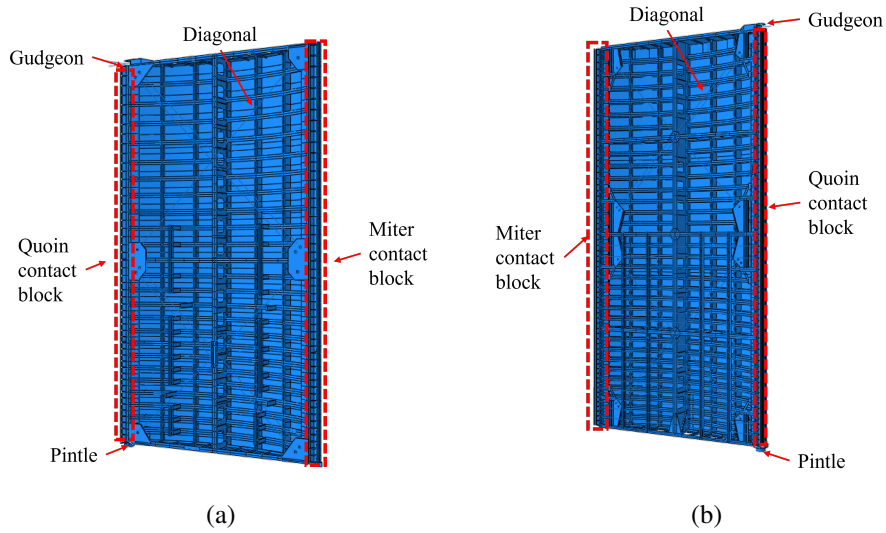


Figure 1. Schematic and main components for the miter gates.(a) Bonneville (b) Dalles

ment (U_1) at the miter contact block was constrained to simulate contact with the adjacent gate leaf; at the pintle located at the bottom, all translational degrees of freedom were restricted ($U_1 = U_2 = U_3 = 0$); at the gudgeon anchorage located at the top, all translations and two rotational degrees of freedom were fixed ($U_1 = U_2 = U_3 = UR_1 = UR_2 = 0$). Along the quoin block, horizontal and vertical displacements ($U_1 = U_2 = 0$) were constrained in the Bonneville model.

Damage Modeling

Two types of damages were considered in the simulation: *gap* and *uniform corrosion*. Gap damage refers to a loss of physical contact between the gate and the wall. In the FE model, the gap is represented by removing the constraints previously described in the quoin block near the bottom of the gate [8], as illustrated in Fig. 2(a).

To simulate uniform corrosion damage, the entire gate structure was divided into three distinct zones based on exposure condition, as shown in Fig. 2(b). For each zone, corrosion was modeled by uniformly reducing the thickness of shell elements. Within each zone, all structural components experienced the same level of thickness reduction, while different reduction values were assigned to reflect varying corrosion severity across the zones.

Strain Gauge Monitoring Data Generation

To simulate realistic strain gauge readings, local partitioning was applied at specific locations on the FE model matching the positions of actual sensors. The material orientation in each region was defined such that the local strain component E_{11} aligned with the physical sensing direction of the strain gauge. A total of 32 sensors were placed in the Dalles model and 40 in the Bonneville model. Fig. 3 shows the sensor locations on both gate models. The finite element simulation employed in this study has been validated against real-world strain gauge measurements, as described in Fillmore et al. [9]. Based on this validation, the simulated data are used for subsequent analysis. The input parameters used to generate the strain gauge data include: (1) Gap length (g); (2) Uniform corrosion thickness reduction in the bottom zone ($T1$); and (3) Upstream and

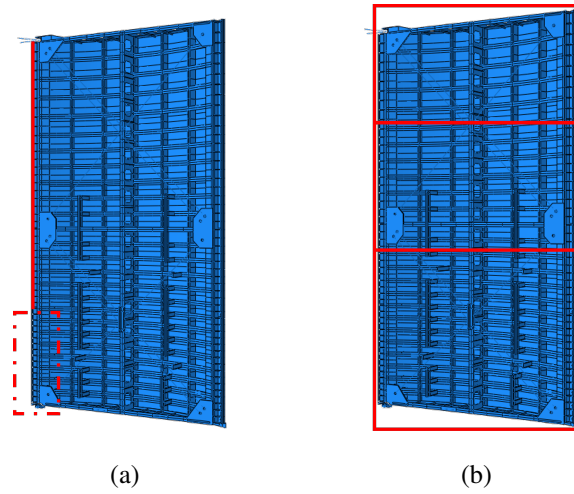


Figure 2. Damage modeling strategies for the miter gate.(a) Free boundary condition to simulate gap damage (b) Three zones for simulate uniform corrosion

downstream water levels (H_{up} and H_{down}).

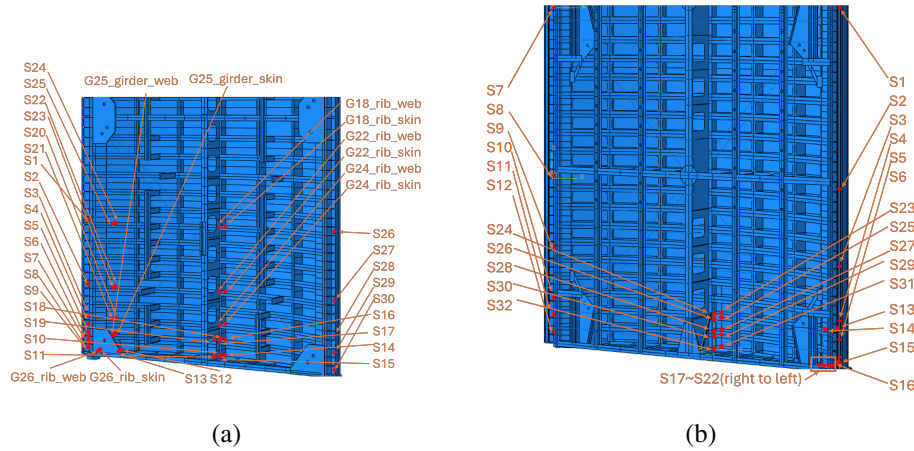


Figure 3. Locations of simulated strain gauges in the finite element models. (a) Bonneville (b) Dalles

All parameters were sampled within their ranges using a Sobol sequence, resulting in 256 simulation cases for each gate model. Tab. I summarizes the input parameter ranges. The strain values (E_{11}) at the sensor locations were used as the output variable.

A sensitivity analysis was performed on the output results to identify sensors that are most responsive to different types of damage. The sensors with high sensitivity to damage were then selected for use in subsequent studies.

DOMAIN ADAPTATION THROUGH DOMAIN ADVERSARIAL NEURAL NETWORK

In this study, we define the Dalles gate as the source structure and the Bonneville gate as the target structure. The sensor data is available for both structures while the damage label is available for only the source structure. Our goal is to predict the absent

TABLE I. Input parameter ranges.

Model	H_{up} (in)	H_{down} (in)	g (in)	T_1 (in)
Dalles	(1101.57, 1259.25)	(105.75, 263.25)	(0, 255.2)	(0, 0.3)
Bonneville	(772.83, 930.31)	(135.02, 292.5)	(0, 220.2)	(0, 0.3)

damage label in the target domain. We only use the target damage label for validation purpose.

Instead of adapting measurements between structures, we aim to generalize damage features across different structures with subsequent mapping to the damage status to guide information transfer. First, damage features are extracted from both source structures and target structures. Then, damage features from the different structures are generalized to the generalized feature and mapped to different damage statuses. By generalizing the damage features, the relationship between damage features and damage labels from source structures is shared with target structures. The concept is to capture damage similarities by identifying commonalities between damage features across different structures. The commonality is a generalization of independent damage feature and can indicate damage status for similar, yet distinct, structures.

Two different functions, i.e., the generalizer and the distinguisher, are needed in the proposed approach. The first serves to generalize damage features and the second serves to distinguish damage severities. Given its dual purpose to generalize features and distinguish damage severities, the functions cannot be completed using traditional data-driven approaches. Drawing from the concept of generative adversarial network (GAN), in which the generator competes with the discriminator [10], we also aim to use competition to achieve generalization. Moreover, the generalizer is connected to a distinguisher as the generalization should be guided by diagnostic mapping. A modified GAN structure called the domain adversarial neural network (DANN) [11] satisfies our requirements.

As Fig. 4 shows, we can obtain guided feature generalization with three connected neural networks. We denote labeled source and unlabeled target structures as L and U , respectively. We first use a feature generalizer to map both damage features from strain gage data, F^L and F^U , to generalized features, G^L and G^U , with a domain classifier network to compete with the generalizer network for the purpose of generalizing. Meanwhile, we train a damage distinguisher network from G^L to the damage label D^L to guide the generalizer network with diagnostic information.

MULTI-DAMAGE DIAGNOSIS RESULTS

We begin by demonstrating multi-damage diagnosis on the labeled source gate before extending the approach to the unlabeled target gate. The diagnostic results for both gap and uniform corrosion on the labeled Dalles gate are presented in Fig. 5. In each plot, the normalized true damage status is shown on the x-axis, while the corresponding normalized predicted damage status is shown on the y-axis. The ideal prediction—where predicted values equal true values—is indicated by the red dashed line. The results indicate accurate predictions for both gap and uniform corrosion.

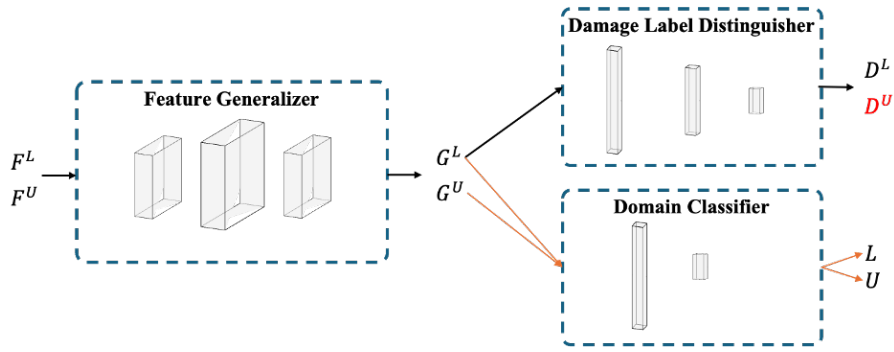


Figure 4. The architecture of the proposed generalized diagnostics network.

TABLE II. Multi-damage diagnosis accuracy comparison for gap and corrosion prediction.

Training Scenario and Evaluation	Gap MSE	Corrosion MSE
Trained on Labeled Source Gate Data Only – Tested on Source Gate Measurement	0.005	0.011
Trained on Labeled Source Gate Data Only – Tested on Target Gate Measurement	0.069	0.221
Trained on Labeled Source + Unlabeled Target Gate Data with Feature Generalization – Tested on Target Gate Measurement	0.015	0.114

In contrast, Fig. 6 illustrates the diagnostic results obtained when directly applying the neural network—trained solely on source structure measurements and labels—to diagnose damage on the unlabeled target structure without feature generalization. The MSE results in Table II also show that the MSE in the predictions for both gap and uniform corrosion is large, highlighting the necessity of domain adaptation techniques.

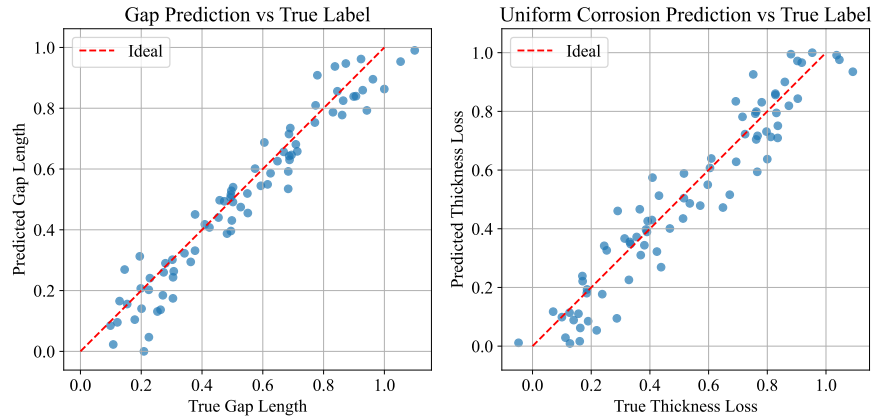


Figure 5. The multi-damage diagnosis results in the test set of Dalles (source) gate.

Fig. 7 presents the multi-damage diagnosis results achieved using the proposed dam-

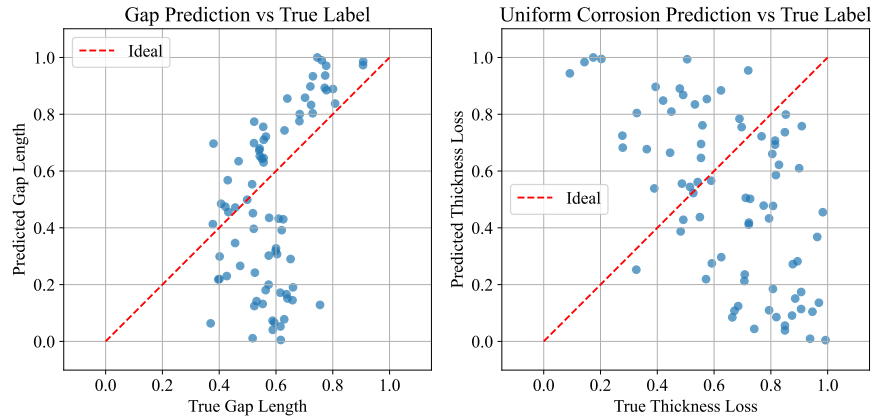


Figure 6. The multi-damage diagnosis results in Bonneville (target) gate without feature generalization.

age feature generalization method. It can be observed that most gap predictions for the target gate are highly accurate. In comparison, the predictions for uniform corrosion capture the overall trend but exhibit reduced accuracy. This discrepancy likely arises from the complex physical effects associated with uniform corrosion, where the relative strain variations across different sensor locations are subtle due to nearly uniform thickness reductions. Overall, the diagnostic accuracy using the feature generalization method significantly improves compared to the scenario without feature generalization as shown from the mean square error from Table II.

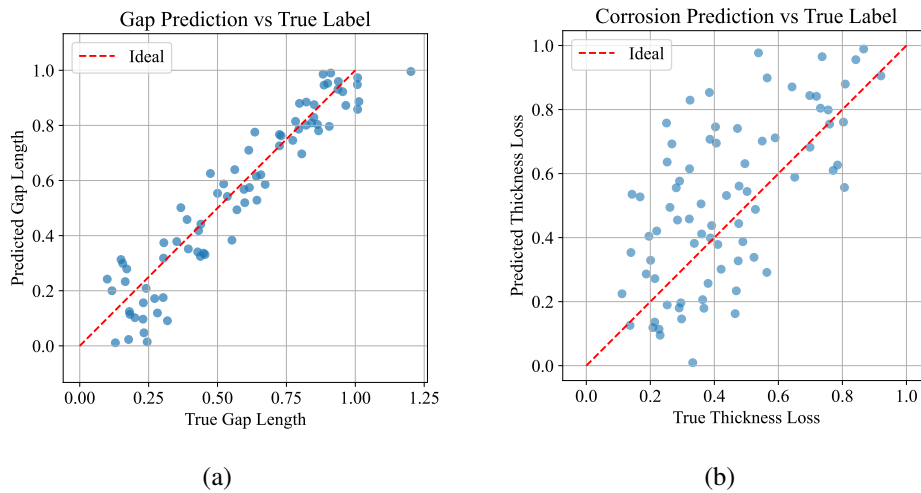


Figure 7. The multi-damage results for Bonneville (target) gate.

CONCLUDING REMARKS

The primary objective of this study is to leverage diagnostic insights from a well-studied miter gate—where multiple damage states are labeled—to diagnose similar but less-studied miter gates with unlabeled damage conditions. The proposed damage fea-

ture generalization approach significantly enhances diagnostic accuracy compared to the scenario without shared information. However, certain damage types exhibit reduced diagnostic accuracy, likely because differing physical characteristics of each damage type affect both their detectability and the effectiveness of knowledge transfer.

ACKNOWLEDGMENT

Funding for this work was provided by the US Army Corps of Engineers through the U.S. Army Engineer Research and Development Center Research Cooperative Agreement W9132T-22-20014. The support is gratefully acknowledged.

REFERENCES

1. Farrar, C. R. and K. Worden. 2012. *Structural Health Monitoring: A Machine Learning Perspective*, John Wiley & Sons, ISBN 978-1-118-44321-7, google-Books-ID: 2w_sp6lrsUC.
2. Gardner, P., L. A. Bull, J. Gosliga, N. Dervilis, and K. Worden. 2021. "Foundations of population-based SHM, Part III: Heterogeneous populations – Mapping and transfer," *Mechanical Systems and Signal Processing*, 149:107142, ISSN 0888-3270, doi:10.1016/j.ymssp.2020.107142.
3. Bull, L. A., P. A. Gardner, J. Gosliga, T. J. Rogers, N. Dervilis, E. J. Cross, E. Papatheou, A. E. Maguire, C. Campos, and K. Worden. 2021. "Foundations of population-based SHM, Part I: Homogeneous populations and forms," *Mechanical Systems and Signal Processing*, 148:107141, ISSN 0888-3270, doi:10.1016/j.ymssp.2020.107141.
4. U.S. Army Corps of Engineers, Portland District, "Bonneville Lock and Dam," <https://www.nwp.usace.army.mil/locks/bonneville-dam/>, accessed: April 25, 2025.
5. U.S. Army Corps of Engineers, Portland District, "The Dalles Lock and Dam," <https://www.nwp.usace.army.mil/locks/the-dalles/>, accessed: April 25, 2025.
6. Wang, S., C. Rodgers, T. Fillmore, B. Welsh, T. Golecki, S. A. V. Shajihan, B. A. Eick, and B. F. Spencer. 2023. "Vision-based model updating and evaluation of miter gates on inland waterways," *Engineering Structures*, 280:115674, ISSN 0141-0296, doi:https://doi.org/10.1016/j.engstruct.2023.115674.
7. Gruben, M. 2019, "Bonneville Lock Closure a 'break in supply chain' for wheat to local ports," https://tdn.com/news/local/bonneville-lock-closure-a-break-in-supply-chain-for-wheat-to-local-ports/article_8ca868ce-1a5c-52db-b0e1-a05d12fb0e54.html, accessed: April 25, 2025.
8. Vega, M. A. 2020. *Diagnosis, prognosis, and maintenance decision making for civil infrastructure*, Ph.D. thesis, University of California, San Diego.
9. Fillmore, T. B., S. Wang, C. Thurmer, B. A. Eick, and B. F. Spencer Jr. 2024. "Multi-modal model updating of miter gates on navigational locks," *Structural Health Monitoring*, 0(0):14759217241290439, doi:10.1177/14759217241290439.
10. Goodfellow, I. J., J. Pouget-Abadie, M. Mirza, B. Xu, D. Warde-Farley, S. Ozair, A. Courville, and Y. Bengio. 2014. "Generative adversarial nets," *Advances in neural information processing systems*, 27.
11. Ganin, Y., E. Ustinova, H. Ajakan, P. Germain, H. Larochelle, F. Laviolette, M. March, and V. Lempitsky. 2016. "Domain-Adversarial Training of Neural Networks," *Journal of Machine Learning Research*, 17(59):1–35, ISSN 1533-7928.